Electrical Power and Energy Systems 155 (2024) 109673

Contents lists available at ScienceDirect

International Journal of Electrical Power and Energy Systems

journal homepage: www.elsevier.com/locate/ijepes

Robust fault estimation for wind turbine pitch and drive train systems

Abdesamia Azizi [a], Tewfik Youssef [a], Abdelmalek Kouadri [a,*], Majdi Mansouri [b], Mohamed Fouzi Mimouni [c]

[a] Signals and systems laboratory, Institute of Electrical and Electronic Engineering, University M'Hamed Bougara of Boumerdes, 35000, Boumerdes, Algeria
[b] Electrical and Computer Engineering Program, Texas A&M University at Qatar, 23874, Doha, Qatar
[c] Automatic, Systems Electrics and Environment (LAS2E)", National School of Engineers of Monastir, University of Monastir, 5019, Monastir, Tunisia

ARTICLE INFO

Keywords:
Wind turbine
Augmented state
Unknown input observer (UIO)
Multi-objective function
Genetic algorithm optimizer

ABSTRACT

The reliability and accuracy of the wind conversion system largely depend on the early detection and diagnosis of faults. In this paper, a novel fault estimator for wind turbine pitch and drive train systems is developed. The main objective is to estimate actuator and sensor faults along with the system states while mitigating the impact of process disturbances and noises. To accomplish this, an augmented state is created by combining the states of the system and different faults. Subsequently, an Unknown Input Observer (UIO) is developed to estimate them simultaneously. The UIO matrices are obtained by optimizing a multi-objective function formed by transforming states and faults estimation errors into the frequency domain using a genetic algorithm. Compared with other approaches, particularly H_∞, the proposed technique shows great superiority in accurately estimating various actuators and sensors faults.

1. Introduction

Humanity has long witnessed incessant technological development that continues to influence all sectors of life. A new technological approach to life has been adopted and as a result, our lives have become easier and more challenging. The price of this advancement is the constant need for energy which is the principal fuel for technology to keep operating and developing. Therefore, the global demand for energy is increasing day by day with the integration of more and more technologies into our daily lives and with the expansion of industrial activities. Coal and oil have been the two main energy sources for decades since the early stages of technological development [1]. But recently, the search for alternative energy sources has become a significant topic in the energy field. Most countries have passed legislation to increase the use of renewable energy sources [2].

Wind energy, a type of sustainable energy, is one of the main energy production techniques that can help achieve this goal. The International Energy Agency (IEA) has published that in 2022, wind power generated more than 2100 terawatt–hours (tWh) representing the second highest growth of all renewable technologies [3]. This catalytic role that wind energy plays in achieving global energy security has placed more attention on the maintenance and repair of wind turbines and called for the need to improve technologies and methods that can help address the challenges and obstacles that wind turbines might face.

Faults in wind turbines require maintenance and/or replacement procedures that reduce energy output. Besides, a component failure can occasionally affect other components, as well as the entire wind turbine. Therefore, it is essential to quickly identify and isolate wind turbine problems and to take the necessary precautions to avoid such undesirable outcomes [4]. The pitch and drive train systems of a wind turbine are crucial components. The pitch system regulates the angle of the wind turbine blades to maintain the gathered wind power near the rated value above the rated wind speed, providing the advantages of better control flexibility and power quality [5]. However, the drive train system is in charge of transferring rotational energy from the turbine blades to the generator. So,the wind turbine pitch and drive train systems must be carefully designed, operated, and maintained to achieve the best performance and dependability. Additionally, to improve wind turbine reliability, a monitoring system should be properly conceived to detect and identify faults and prevent them from causing serious damage or downtime. In addition, it can enable wind turbines to operate normally even in the presence of faults which is known as fault-tolerant control.

Fault estimation is an important step in fault-tolerant control because it allows one to estimate the magnitude, shape, and location of a fault that occurs. This could be a fault in a system component, sensor, or actuator. In general, fault estimation is performed by designing an observer based on the system's mathematical model. Many works have been done regarding the design of an observer-based actuator and sensor fault estimation for wind turbine pitch and drive train

* Corresponding author.
E-mail address: ab_kouadri@hotmail.com (A. Kouadri).

https://doi.org/10.1016/j.ijepes.2023.109673
Received 5 June 2023; Received in revised form 26 October 2023; Accepted 16 November 2023
Available online 29 November 2023

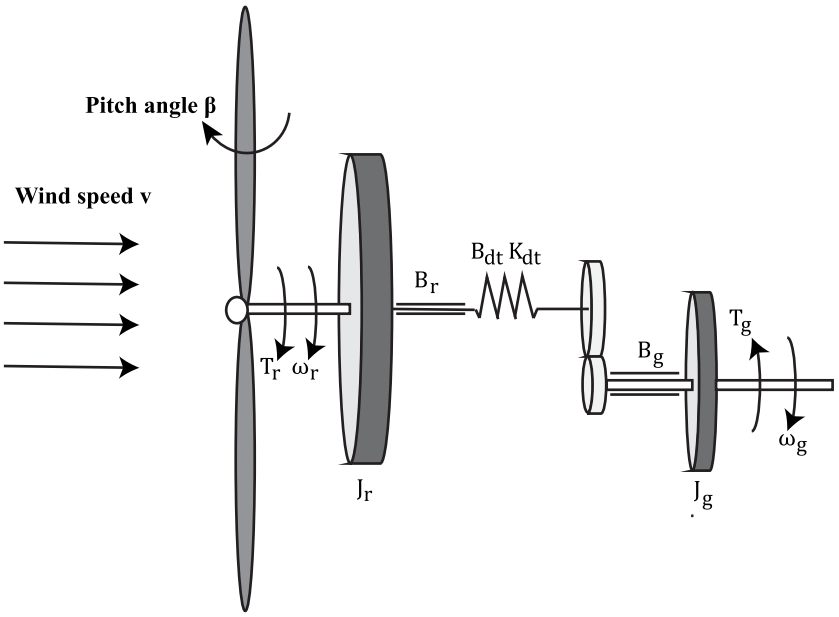

Fig. 1. Mechanical scheme of the wind turbine transmission system.

systems [6–11]. Reconstructing faults in a system while accounting for disturbances and noise presents a significant challenge in fault estimation. To overcome this issue, various approaches have been developed. One such approach is to perform a multitude of optimization computations to create a residual that is responsive to faults while being unsusceptible to disturbances and/or uncertainty [12–21]. The decoupling strategy eliminates disturbances from the estimate error dynamics, provided that the distribution matrix meets the matching rank criteria. This technique has been employed in studies by [22–24]. Authors in [25] presented an unknown input observer that decouples partial disturbances and attenuates the remaining disturbances using H_∞ optimization. Finally, the reconstruction approach estimates perturbation effects and removes them, as discussed and reported in [26–28]. In this work, the wind turbine pitch and drive train systems are jointly modeled in state space representation. An augmented representation is then created by incorporating the system states and faults into an augmented state vector. An Unknown Input Observer (UIO) is then introduced to estimate this augmented state vector which consists of system states, actuator and sensor faults. To ensure robust fault estimation against disturbances and output noise, a genetic algorithm is used to determine the different UIO gain matrices by minimizing a multi-objective function formed by various performance indices described in the frequency domain. So, the main contribution of this paper is a novel approach to finding UIO gain matrices for wind turbine pitch and drive train systems using a genetic algorithm optimizer, to mitigate disturbances, and reduce their impact on the estimation process, without making assumptions about the rank of the disturbance matrix.

The remaining sections of this paper are organized as follows: Section 2 describes the wind turbine pitch and drive train model. Section 3 discusses the architecture of the unknown input observer. Section 4 discusses obtaining UIO gain matrices using the proposed and with H_∞ approaches. A simulation example is provided in Section 5, and Section 6 draws some conclusions.

2. Wind turbine pitch and drive train model

For a pitch system, a second-order closed-loop transfer function from β_{ref} (the pitch reference angle) to pitch angle β is used to describe the hydraulic pitch actuator [29]:

$$\frac{\beta(s)}{\beta_{ref}(s)} = \frac{\omega_n^2}{s^2 + 2\xi\omega_n s + \omega_n^2} \tag{1}$$

where ξ and ω_n represent the damping factor and natural frequency, respectively. The state space equation of the transfer function (1) is given as follows (2):

$$\begin{bmatrix}\dot{\beta}(t)\\ \ddot{\beta}(t)\end{bmatrix} = \begin{bmatrix}0 & 1\\ -\omega_n^2 & -2\xi\omega_n\end{bmatrix}\begin{bmatrix}\beta(t)\\ \dot{\beta}(t)\end{bmatrix} + \begin{bmatrix}0\\ \omega_n^2\end{bmatrix}\beta_{ref}(t) \tag{2}$$

The drive train system is composed of a low-speed shaft and a high-speed shaft, which have inertia J_r and J_g and friction coefficients B_r and B_g, respectively. The connection between the two shafts is made through a transmission that has a gear ratio N_g and efficiency η_{dt} and also features torsion stiffness K_{dt} and torsion damping B_{dt} [30]. In summary, the drive train system can be represented by the following three differential equations:

$$\begin{cases}\dot{\omega}_r(t) = -\dfrac{B_{dt}+B_r}{J_r}\omega_r(t) + \dfrac{B_{dt}}{N_g J_r}\omega_g(t) - \dfrac{K_{dt}}{J_r}\theta_\Delta(t) + \dfrac{T_r(t)}{J_r}\\ \dot{\omega}_g(t) = \dfrac{\eta_{dt}B_{dt}}{N_g J_g}\omega_r(t) - \left(\dfrac{\eta_{dt}B_{dt}}{N_g^2 J_g} + \dfrac{B_g}{J_g}\right)\omega_g(t) + \dfrac{\eta_{dt}K_{dt}}{N_g J_g}\theta_\Delta(t) - \dfrac{T_g(t)}{J_g}\\ \dot{\theta}_\Delta(t) = \omega_r(t) - \dfrac{\omega_g(t)}{N_g}\end{cases} \tag{3}$$

where ω_r and ω_g are the rotor and generator speeds in rad/s, respectively. θ_Δ is the torsion angle of the drive train in rad. T_r and T_g are the aerodynamic and generator torques in $\mathrm{N}\cdot\mathrm{m}$, respectively (see Fig. 1). The aerodynamic torque applied to the rotor is given as [31]:

$$T_r(t) = \frac{P_r}{\omega_r} \tag{4}$$

where P_r is the mechanical power captured by the wind turbine defined as:

$$P_r = \frac{1}{2}\rho\pi R_b^2 v^3 C_p(\lambda,\beta)$$

R_b is the length of the fan blades, ρ is the air density, v is the wind speed, and $C_p(\lambda,\beta)$ is the wind energy conversion coefficient, which depends on the tip speed ratio λ and pitch angle β. $C_p(\lambda,\beta)$ and λ are expressed as follows as in [11]:

$$\lambda = \frac{\omega_r R_b}{v} \tag{5}$$

$$\frac{1}{\lambda_i} = \frac{1}{\lambda + 0.08\beta} - \frac{0.0035}{\beta^3 + 1} \tag{6}$$

Table 1
Different system parameters.

Parameter	Value	Parameter	Value
J_r	55×10^6 kg · m^2	η_{dt}	0.97
τ_g	20×10^{-3} s	ρ	1.225 kg/m^3
J_g	390 kg · m^2	K_{dt}	2.7×10^9 N · m/rad
ω_n	11.11 rad/s	R_b	57.5 m
B_r	7.11 N · m · s/rad	B_{dt}	775.49 N · m · s/rad
ξ	0.6	B_g	45.6 N · m · s/rad
N_g	95		

$$C_p(\lambda,\beta)=0.5176\left(\frac{116}{\lambda_i}-0.4\beta-5\right)e^{-\frac{21}{\lambda_i}}+0.0068\lambda \tag{7}$$

The reference torque $T_{g,ref}$ controls the generator torque T_g. A first-order model (8) with the time constant τ_g approximates the dynamics [32]:

$$\dot{T}_g(t)=-\frac{T_g(t)}{\tau_g}+\frac{T_{g,ref}(t)}{\tau_g} \tag{8}$$

The two subsystems (2) and (3) are gathered in the state space representation as follows:

$$\begin{cases}\dot{x}=Ax+Bu\\ y=Cx\end{cases} \tag{9}$$

where $x=\begin{bmatrix}\omega_r & \omega_g & \theta_\Delta & \beta & \dot{\beta}\end{bmatrix}^T$, $u=\begin{bmatrix}T_r & T_g & \beta_{ref}\end{bmatrix}^T$, $C=\begin{bmatrix}1&0&0&0&0\\0&1&0&0&0\\0&0&0&1&0\end{bmatrix}$

$$A=\begin{bmatrix}-\frac{B_{dt}+B_r}{J_r} & \frac{B_{dt}}{N_gJ_r} & -\frac{K_{dt}}{J_r} & 0 & 0\\ \frac{\eta_{dt}B_{dt}}{N_gJ_g} & -\left(\frac{\eta_{dt}B_{dt}}{N_g^2J_g}+\frac{B_g}{J_g}\right) & \frac{\eta_{dt}K_{dt}}{N_gJ_g} & 0 & 0\\ 1 & -\frac{1}{N_g} & 0 & 0 & 0\\ 0 & 0 & 0 & 0 & 1\\ 0 & 0 & 0 & -\omega_n^2 & -2\xi\omega_n\end{bmatrix},$$

$$B=\begin{bmatrix}\frac{1}{J_r} & 0 & 0\\ 0 & -\frac{1}{J_g} & 0\\ 0&0&0\\0&0&0\\0&0&\omega_n^2\end{bmatrix}$$

The superscript T denotes the transpose of a matrix.

Table 1 shows the different values of the system parameters used in this paper, which were derived from [32].

3. Observer design

Assume that system (9) is subjected to external and undesirable inputs as follows:

$$\begin{cases}\dot{x}=Ax+B\begin{bmatrix}T_r+\Delta T_r\\ T_g+\Delta T_g\\ \beta_{ref}\end{bmatrix}\\ y=C\begin{bmatrix}\omega_r+\Delta\omega_r\\ \omega_g\\ \theta_\Delta\\ \beta+\Delta\beta\\ \dot{\beta}\end{bmatrix}+\eta\end{cases} \tag{10}$$

Where ΔT_g is an actuator fault, ΔT_r is treated as disturbances, $\Delta\omega_r$ and $\Delta\beta$ are sensor faults, and η is the measurement noises. By developing

$$B\begin{bmatrix}T_r+\Delta T_r\\ T_g+\Delta T_g\\ \beta_{ref}\end{bmatrix}=B\begin{bmatrix}T_r\\ T_g\\ \beta_{ref}\end{bmatrix}+B\begin{bmatrix}\Delta T_r\\ \Delta T_g\\ 0\end{bmatrix}$$

$$=B\begin{bmatrix}T_r\\ T_g\\ \beta_{ref}\end{bmatrix}+\begin{bmatrix}\frac{1}{J_r}\\0\\0\\0\\0\end{bmatrix}\Delta T_r+\begin{bmatrix}0&0&0\\-1/J_g&0&0\\0&0&0\\0&0&0\\0&0&0\end{bmatrix}\begin{bmatrix}f_a\\f_s\end{bmatrix}$$

furthermore,

$$C\begin{bmatrix}\omega_r+\Delta\omega_r\\ \omega_g\\ \theta_\Delta\\ \beta+\Delta\beta\\ \dot{\beta}\end{bmatrix}=C\begin{bmatrix}\omega_r\\ \omega_g\\ \theta_\Delta\\ \beta\\ \dot{\beta}\end{bmatrix}+\begin{bmatrix}\Delta\omega_r\\0\\\Delta\beta\end{bmatrix}$$

$$=Cx+\begin{bmatrix}1&0\\0&0\\0&1\end{bmatrix}\begin{bmatrix}\Delta\omega_r\\\Delta\beta\end{bmatrix}$$

$$=Cx+\begin{bmatrix}0&1&0\\0&0&0\\0&0&1\end{bmatrix}\begin{bmatrix}f_a\\f_s\end{bmatrix}$$

where $f_a=\Delta T_g$ and $f_s=\begin{bmatrix}\Delta\omega_r\\\Delta\beta\end{bmatrix}$, Eq. (10) is rewritten as shown below:

$$\begin{cases}\dot{x}=Ax+Bu+F_df+Dd\\ y=Cx+F_mf+\eta\end{cases} \tag{11}$$

where $f=\begin{bmatrix}f_a^T & f_s^T\end{bmatrix}^T$, f_a and f_s are actuator and sensor faults, respectively. $d=\Delta T_r$, $D=\begin{bmatrix}\frac{1}{J_r}&0&0&0&0\end{bmatrix}^T$, $F_d=\begin{bmatrix}0&-\frac{1}{J_g}&0&0&0\\0&0&0&0&0\\0&0&0&0&0\end{bmatrix}^T$, and $F_m=\begin{bmatrix}0&1&0\\0&0&0\\0&0&1\end{bmatrix}$.

3.1. Augmented system

For the more general case, let $\mathbb{R}^n,\mathbb{R}^m,\mathbb{R}^{n_f},\mathbb{R}^{n_d}$, and $\mathbb{R}^p$ be the dimensions of x,u,f,d, and y, respectively; Let the augmented state vector $x_a\in\mathbb{R}^{n_a}$ be as in [18]:

$$x_a=\begin{bmatrix}x^T & \dot{f}^T & f^T\end{bmatrix}^T \tag{12}$$

where $n_a=n+2\cdot n_f$. In addition, the second derivative of fault $\ddot{f}$ is supposed to be not null [33], i.e., $\ddot{f}\neq0$.

Thus, the state space representation (11) is rewritten in an augmented state space form as follows:

$$\begin{cases}\dot{x}_a=A_ax_a+B_au+D_ad+F\ddot{f}\\ y=C_ax_a+\eta\end{cases} \tag{13}$$

where

$$A_a=\begin{bmatrix}A&0&F_d\\0&0&0\\0&I&0\end{bmatrix},B_a=\begin{bmatrix}B\\0\\0\end{bmatrix},D_a=\begin{bmatrix}D\\0\\0\end{bmatrix},F=\begin{bmatrix}0\\I\\0\end{bmatrix},C_a=\begin{bmatrix}C&0&F_m\end{bmatrix} \tag{14}$$

and I is an identity matrix with appropriate dimension.

Remark 1. x_a obviously contains the state vector x, the relevant fault vector f, and its first-order derivative $\dot{f}$. As a result, the estimation of x_a leads to estimating the three components, simultaneously.

3.2. Unknown input observer

Consider the following proportional unknown input observer as in [34]:

$$\begin{cases}\dot{z}=Mz+Nu+Gy\\ \hat{x}_a=z+Hy\end{cases} \tag{15}$$

where $z \in R^{n_a}$ is the state vector of the dynamic system (15), $\hat{x}_a$ is the estimation of x_a, while M, N, G and H are the observer gain matrices to be determined.

Let the estimation error be, $e = x_a - \hat{x}_a$, by using (15) we will have:

$$\begin{aligned} e &= x_a - \hat{x}_a \\ &= x_a - z - HC_a x_a - H\eta \\ &= (I - HC_a)x_a - z - H\eta \end{aligned} \tag{16}$$

From (16), one can get:

$$z = (I - HC_a)x_a - e - H\eta \tag{17}$$

Consequently, by using Eqs. (13), (15), (16) and (17), the estimation error derivative is as follows:

$$\begin{aligned} \dot{e} &= (I - HC_a)\dot{x}_a - \dot{z} - H\dot{\eta} \\ &= (I - HC_a)(A_a x_a + B_a u + D_a d + F\ddot{f}) - (Mz + Nu + GC_a x_a + G\eta) \\ &\quad - H\dot{\eta} \\ &= [(I - HC_a)A_a - GC_a - M(I - HC_a)]x_a + [(I - HC_a)B_a - N]u \\ &\quad + (I - HC_a)D_a d + (I - HC_a)F\ddot{f} + Me - (G - MH)\eta - H\dot{\eta} \end{aligned} \tag{18}$$

If the below relations can be maintained:

$$(I - HC_a)A_a - GC_a - M(I - HC_a) = 0 \tag{19}$$

$$(I - HC_a)B_a - N = 0 \tag{20}$$

and by rewriting (19) as:

$$M = A_a - KC_a - HC_a A_a \tag{21}$$

where $K = G - MH$ (22)

The estimation error derivative (18) becomes:

$$\dot{e} = Me + (I - HC_a)D_a d + (I - HC_a)F\ddot{f} - K\eta - H\dot{\eta} \tag{23}$$

Under the absence of external inputs ($d = 0, \ddot{f} = 0$, and $\eta = 0$), the estimation error is stable if and only if the matrix M is **hurwitz**.

The necessary and sufficient conditions for the existence of the (UIO) (15) for the system (11) are established under the following assumptions:

Assumption 1. The pair (A, C) is observable.

Assumption 2. $\begin{bmatrix} A & F_d \\ C & F_m \end{bmatrix}$ is full column rank.

Remark 2. Assumption 1 is commonly adopted for observers to ensure system states observability [26]. Additionally, Assumption 2 can be understood as the need for the transmission zeros stemming from the unknown inputs to the measurements to be in a stable state [25].

4. UIO gain matrices

4.1. Proposed using genetic algorithm

The main objective of this work is to design the previous UIO (15) in such a way that the transfer function between the estimation error and each input (disturbances, noises, and the second derivative of a fault) has its maximum singular value minimized, meaning that its infinite norm is minimal.

Applying Laplace transform to Eq. (23), with null initial conditions, the relation between estimation error and the different inputs is as follows:

$$\begin{aligned} e(s) &= (sI - M)^{-1}(I - HC_a)D_a d(s) - (sI - M)^{-1}(K + Hs)\eta(s) \\ &\quad + (sI - M)^{-1}(I - HC_a)Fs^2 f(s) \end{aligned} \tag{24}$$

The following performance indices to be minimized are proposed [33, 35]:

$$T_1(K, H) = \|(sI - A_a + KC_a + HC_a A_a)^{-1}(I - HC_a)D_a\|_{s=jw_d} \tag{25}$$

$$T_2(K, H) = \|(sI - A_a + KC_a + HC_a A_a)^{-1}(K + Hs)\|_{s=jw_\eta} \tag{26}$$

$$T_3(K, H) = \|(sI - A_a + KC_a + HC_a A_a)^{-1}(I - HC_a)Fs^2\|_{s=jw_f} \tag{27}$$

where $\|\cdot\|$ denotes the infinite norm. w_d, w_η, and w_f are the disturbance, noise, and the second derivative of fault dominant frequencies, respectively.

By minimizing T_1, T_2, and T_3, the effect of disturbances, noises, and the second derivative of faults on the estimation error will be reduced, respectively.

The Weighted Sum Multi-objective function to be assessed is as follows:

$$\begin{aligned} &\underset{K,H}{\text{minimize}} \quad \sum_{i=1}^{3} \alpha_i T_i(K, H) \\ &\text{subject to} \quad real(\lambda(A_a - KC_a - HC_a A_a)) < 0 \end{aligned} \tag{28}$$

where $0 < \alpha_i \leq 1$ and $\sum_{i=1}^{3} \alpha_i = 1$, and $real(\lambda(\xi))$ is the real part of ξ's eigenvalues.

To remove the constraint of the objective function (28), the matrices K and H are rewritten in terms of the estimation error state matrix's eigenvalues.

Assume that there are n_r real eigenvalues $\lambda_i (i = 1 \quad \cdots \quad n_r)$, and n_c pairs of complex-conjugate eigenvalues $\lambda_{i,re} \pm j\lambda_{i,img} (i = 1 \quad \cdots \quad n_c)$ and that any of n_r and n_c meet the relation:

$$n_r + 2n_c = n_a \tag{29}$$

The relationship between the closed-loop observer matrix $(A_a - K \cdot C_a - H \cdot C_a \cdot A_a)$ eigenvalues and eigenvectors can be represented as:

$$(A_a - KC_a - HC_a A_a)^T v_i = \lambda_i v_i, \quad i = 1, 2, \ldots, n_a \tag{30}$$

where λ_i is the right eigenvalue of the closed-loop observer matrix $(A_a - KC_a - HC_a A_a)^T$ and v_i is the corresponding eigenvector of λ_i, and $i = 1 \quad \cdots \quad n_a$.

For real eigenvalues, $(i = 1 \quad \cdots \quad n_c)$, we can express the eigenvectors v_i as follows:

$$(A_a^T - C_a^T K^T - A_a^T C_a^T H^T)v_i = \lambda_i v_i \tag{31}$$

or

$$v_i = -(\lambda_i I - A_a^T)^{-1} C_a^T q_i - (\lambda_i I - A_a^T)^{-1} A_a^T C_a^T r_i \tag{32}$$

where

$$q_i = K^T v_i \tag{33}$$

$$r_i = H^T v_i \tag{34}$$

In the case where the eigenvalues are complex conjugate:

$$\lambda_i = \lambda_{i,re} + j\lambda_{i,img} \tag{35}$$

$$v_i = v_{i,re} + jv_{i,img} \tag{36}$$

from (30), one can get:

$$(A_a^T - C_a^T K^T - A_a^T C_a^T H^T)(v_{i,re} + jv_{i,img}) = (\lambda_{i,re} + j\lambda_{i,img})(v_{i,re} + jv_{i,img}) \tag{37}$$

This equivalent to:

$$\begin{cases} (A_a^T - C_a^T K^T - A_a^T C_a^T H^T)v_{i,re} = \lambda_{i,re} v_{i,re} - \lambda_{i,img} v_{i,img} \\ (A_a^T - C_a^T K^T - A_a^T C_a^T H^T)v_{i,img} = \lambda_{i,img} v_{i,re} + \lambda_{i,re} v_{i,img} \end{cases} \tag{38}$$

or

$$\begin{cases} (\lambda_{i,re} I - A_a^T)v_{i,re} - \lambda_{i,img} v_{i,img} = -C_a^T K^T v_{i,re} - A_a^T C_a^T H^T v_{i,re} \\ \lambda_{i,img} v_{i,re} + (\lambda_{i,re} I - A_a^T)v_{i,img} = -C_a^T K^T v_{i,img} - A_a^T C_a^T H^T v_{i,img} \end{cases} \tag{39}$$

by making

$$A_{ai} = \begin{bmatrix} (\lambda_{i,re} I - A_a^T) & -\lambda_{i,img} I \\ \lambda_{i,img} I & (\lambda_{i,re} I - A_a^T) \end{bmatrix}, C_1 = \begin{bmatrix} C_a^T & 0 \\ 0 & C_a^T \end{bmatrix},$$
$$C_2 = \begin{bmatrix} A_a^T C_a^T & 0 \\ 0 & A_a^T C_a^T \end{bmatrix}$$

and

$$\begin{cases} q_{i,re} = K^T v_{i,re} \\ q_{i,img} = K^T v_{i,img} \end{cases} \tag{40}$$

$$\begin{cases} r_{i,re} = H^T v_{i,re} \\ r_{i,img} = H^T v_{i,img} \end{cases} \tag{41}$$

we will have the eigenvectors for $i = 1, 2, \ldots, n_c$ as follows:

$$\begin{bmatrix} v_{i,re} \\ v_{i,img} \end{bmatrix} = -A_{a_i}^{-1} C_1 \begin{bmatrix} q_{i,re} \\ q_{i,img} \end{bmatrix} - A_{a_i}^{-1} C_2 \begin{bmatrix} r_{i,re} \\ r_{i,img} \end{bmatrix} \tag{42}$$

The observer gain matrices K and H are given by:

$$K = (QV^{-1})^T \tag{43}$$

$$H = (RV^{-1})^T \tag{44}$$

where

$$\begin{aligned} V &= \begin{bmatrix} v_1 & \cdots & v_{n_r} & v_{1,re} & \cdots & v_{n_c,re} & v_{1,img} & \cdots & v_{n_c,img} \end{bmatrix} \in R^{n_a \times n_a} \\ Q &= \begin{bmatrix} q_1 & \cdots & q_{n_r} & q_{1,re} & \cdots & q_{n_c,re} & q_{1,img} & \cdots & q_{n_c,img} \end{bmatrix} \in R^{p \times n_a} \\ R &= \begin{bmatrix} r_1 & \cdots & r_{n_r} & r_{1,re} & \cdots & r_{n_c,re} & r_{1,img} & \cdots & r_{n_c,img} \end{bmatrix} \in R^{p \times n_a} \end{aligned} \tag{45}$$

Therefore, Eq. (28) becomes:

$$\begin{aligned} &\underset{Q,R,\lambda_1,\ldots,\lambda_{n_a}}{\text{minimize}} \quad \sum_{i=1}^{3} \alpha_i T_i(Q, R, \lambda_1, \ldots, \lambda_{n_a}) \\ &\text{subject to} \quad real(\lambda_i) < 0, \quad i = 1, 2, \ldots, n_a \end{aligned} \tag{46}$$

Furthermore, a new real scalar variable s_i is introduced to remove the above constraint for real eigenvalues using the following formula [36]:

$$\lambda_i = L_i + (U_i - L_i) \cdot \sin^2(s_i) \tag{47}$$

where, $\lambda_i \in [L_i, U_i]$. L_i and U_i are the lower and the upper value of λ_i to be designed, whilst for complex eigenvalues:

$$\lambda_{i,re} = L_{i,re} + (U_{i,re} - L_{i,re}) \cdot \sin^2(s_i) \tag{48}$$

$$\lambda_{i,img} = L_{i,img} + (U_{i,img} - L_{i,img}) \cdot \sin^2(s_i) \tag{49}$$

$$\lambda_i = \lambda_{i,re} \pm j \cdot \lambda_{i,img} \tag{50}$$

where, $\lambda_{i,re} \in [L_{i,re}, U_{i,re}]$ and $\lambda_{i,img} \in [L_{i,img}, U_{i,img}]$. Hence, Eq. (46) becomes:

$$\underset{Q,R,s_1,\ldots,s_{n_a}}{\text{minimize}} \quad \sum_{i=1}^{3} \alpha_i T_i(Q, R, s_1, \ldots, s_{n_a}) \tag{51}$$

The procedure for designing the proposed UIO consists of first creating the augmented system of the form (13), then finding the UIO gain matrices K and H by minimizing (51) using a genetic algorithm, then calculate the rest of the parameters M, N, and G expressed respectively in (19), (21) and (22). The different steps for evaluating the multi-objective function (51) are listed below:

Step 1. Start with initial values of R, Q, and s_i.
Step 2. Calculate the eigenvalues using (47) or (50) after designing the upper and lower bounds.
Step 3. Calculate the eigenvectors using R, Q, and the eigenvalues employing (32) or (42).
Step 4. Calculate K and H using (43) and (44).
Step 5. Finally, evaluate (51) by first calculating the performance indices T_1, T_2, and T_3 in (25), (26) and (27), respectively.

4.2. Using H_∞ optimization

Definition 1. A system is said to be stable with H_∞ performance if the following conditions are satisfied [37]: (1) With zero disturbance, the system is asymptotically stable. (2) With zero initial condition and for a given positive constant γ the following condition holds:

$$\int_0^\infty x^T x \, dt < \gamma^2 \int_0^\infty d^T d \, dt \tag{52}$$

where x and d are the system state vector and the disturbance, respectively.

Lemma 1 (*Schur Complement [38]*). *Let* $P = \begin{bmatrix} P_{11} & P_{12} \\ * & P_{22} \end{bmatrix}$ *be a symmetric matrix, then:*

$$P < 0 \equiv P_{22} < 0 \text{ and } P_{11} - P_{12} P_{22} P_{12}^T < 0$$

Theorem 1. *There exists a robust observer (15) that can be achieve* H_∞ *performance (52), if there exist a symmetric positive definite matrix* $X \in \mathbb{R}^{n_a \times n_a}$ *and a scalar* $\delta > 0$ *satisfying:*

$$\begin{bmatrix} XM + M^T X & (X - Y_2 C_a) D_a & (X - Y_2 C_a) F & -Y_1 & -Y_2 & I_{n_a} \\ * & -\delta I_{n_d} & 0 & 0 & 0 & 0 \\ * & * & -\delta I_{n_f} & 0 & 0 & 0 \\ * & * & * & -\delta I_p & 0 & 0 \\ * & * & * & * & -\delta I_p & 0 \\ * & * & * & * & * & -\delta I_{n_a} \end{bmatrix} < 0 \tag{53}$$

where $Y_1 = XK$, $Y_2 = XH$, *and* $XM = XA_a - Y_1 C_a - Y_2 C_a A_a$.

Proof. Define a Lyapunov function as:

$$V(e) = e^T X e \tag{54}$$

where $X = X^T > 0$. Using (23), the derivative of V with respect to time yields that:

$$\begin{aligned} \dot{V}(e) &= \dot{e}^T X e + e^T X \dot{e} \\ &= \Big(M^T e^T + d^T D_a^T (I - H C_a)^T + \dot{f}^T F^T (I - H C_a)^T \\ &\quad - \dot{\eta}^T K^T - \dot{\eta}^T H^T \Big) X e + \\ &\quad e^T X \Big(M e + (I - H C_a) D_a d + (I - H C_a) F \ddot{f} - K \eta - H \dot{\eta} \Big) \\ &= \begin{bmatrix} e^T & d_s^T \end{bmatrix} \Pi \begin{bmatrix} e \\ d_s \end{bmatrix} \end{aligned} \tag{55}$$

where

$$\Pi = \begin{bmatrix} M^T X + XM & X(I - HC_a) D_a & X(I - HC_a) F & -XK & -XH \\ * & 0 & 0 & 0 & 0 \\ * & * & 0 & 0 & 0 \\ * & * & * & 0 & 0 \\ * & * & * & * & 0 \end{bmatrix},$$

$$d_s = \begin{bmatrix} d \\ \ddot{f} \\ \eta \\ \dot{\eta} \end{bmatrix}$$

Let

$$P_h = \int_0^\infty \delta^{-1} e^T e - \delta d_s^T d_s \, dt \tag{56}$$

by using Eqs. (55) and (56), one can get:

$$\begin{aligned} P_h &= \int_0^\infty \delta^{-1} e^T e - \delta d_s^T d_s + \dot{V}(e) \, dt - \int_0^\infty \dot{V}(e) \, dt \\ &= \int_0^\infty \begin{bmatrix} e^T & d_s^T \end{bmatrix} \Pi_1 \begin{bmatrix} e \\ d_s \end{bmatrix} dt - \int_0^\infty \dot{V}(e) \, dt \end{aligned} \tag{57}$$

$$\Pi_1 = \begin{bmatrix} M^T X + XM + \delta^{-1} I_{n_a} & X(I - HC_a)D_a & X(I - HC_a)F & -XK & -XH \\ * & -\delta I_{n_d} & 0 & 0 & 0 \\ * & * & -\delta I_{n_f} & 0 & 0 \\ * & * & * & -\delta I_p & 0 \\ * & * & * & * & -\delta I_p \end{bmatrix} \tag{58}$$

Box I.

Table 2
Root mean square error between system states, actuator, and sensor faults and their estimation (first case).

Approach	x_1	x_2	x_3	x_4	x_5	f_a	f_{s_1}	f_{s_2}
H_∞	0.0000	0.0009	0.0000	0.0042	**0.0154**	181.2895	0.0014	0.0040
Proposed	0.0000	**0.0008**	0.0000	**0.0039**	0.0243	**14.8411**	**0.0008**	**0.0039**

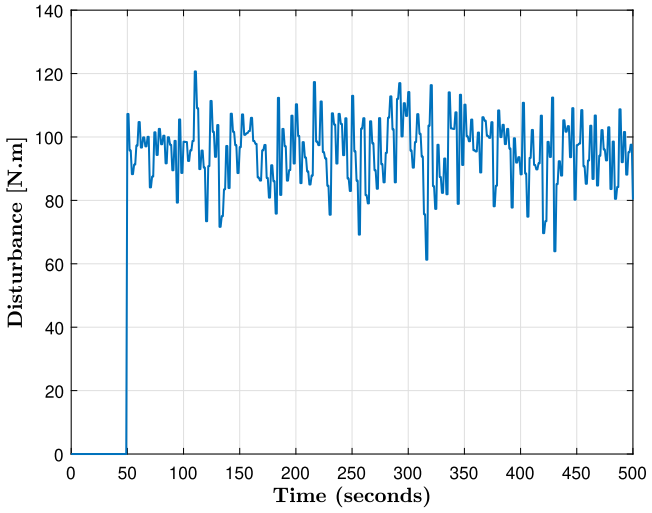

Fig. 2. Disturbance $d_r(t)$.

where (see Eq. (58) in Box I).

Under zero initial condition, $e(0) = 0$:

$$\int_0^\infty \dot{V}(e)\,dt = V(e(\infty)) > 0 \tag{59}$$

$\Pi_1 < 0$ implies that $P_h < 0$, which means

$$\int_0^\infty e^T e\,dt < \int_0^\infty \delta^2 d_s^T d_s\,dt$$

setting $Y_1 = XK$ and $Y_2 = XH$, and utilizing Lemma 1 on Eq. (58), demonstrates Theorem 1.

5. Results and discussion

The simulation is divided into two parts to address the two cases of the disturbances matrix; one where it has a full column rank, and the other where it does not. When comparing the different approaches, the bold value represents the best value of the corresponding variable while the underline values represent the best approach for all variables set.

The weighting factors α_1, α_2, and α_3 presented in Eq. (51) are each considered to be $\frac{1}{3}$.

5.1. Case 1: Not full column rank disturbances matrix

For this simulation of wind turbine pitch and drive train systems, the actuator fault is considered to be random following Weibull distribution with the scale of 1.2×10^3 and shape equal to 8 starting from $t = 100$ s; The noises η affecting the system are Gaussian noises with 0 mean and 10^{-3} standard deviation. The sensor faults f_{s_1} and f_{s_2} are as follows:

$$f_{s_1}(t) = \begin{cases} 0, & t < 300 \\ 0.2 + 0.05\sin(0.3(t - 300)), & t \geq 300 \end{cases}$$

$$f_{s_2}(t) = \begin{cases} 0, & t < 150 \\ \frac{1.8}{50}(t - 150), & 150 \leq t < 200 \\ 1.8 + 0.8\cos(0.2(t - 200))\sin(0.02(t - 200)), & t \geq 200 \end{cases}$$

Regarding the disturbances, additional perturbations have been introduced to achieve a disturbance matrix with a non-full column rank. D is taken as:

$$D = \begin{bmatrix} \frac{1}{J_r} & \frac{-5}{J_r} \\ 0 & 0 \\ 0 & 0 \\ 0 & 0 \\ 0 & 0 \end{bmatrix}$$

and the disturbance $d(t)$:

$$d(t) = \begin{bmatrix} d_r(t) \\ 10^2(u(t - 100) - u(t - 300)) \end{bmatrix}$$

where $u(t)$ is the unit step function and $d_r(t)$ is considered to be random following a Weibull distribution with the scale of 10^3 and shape equal 10 starting from $t = 50$ s as illustrated in Fig. 2.

It can be seen from Figs. 3 to 9, the proposed approach consistently demonstrates higher accuracy in estimating system states and different faults compared to that of H_∞. This highlights the effectiveness of the proposed approach for robust estimation. As shown in Table 2, the suggested strategy outperforms H_∞ in many cases, particularly in estimating faults with random behavior (e.g., the actuator fault shown in Fig. 7). Obviously, the proposed approach achieves an RMSE value of 14.8411, whereas H_∞ yields 181.2895. The different observer gain matrices of the two techniques are provided in Appendix A.

5.2. Case 2: Full column rank disturbance matrix with uncertainties

In this case, we are considering that the system is subject to uncertainties $\zeta(x)$, actuator fault f_a, and the disturbances d:

$$\begin{cases} \dot{x} = Ax + Bu + F_a f_a + Dd + \Xi\zeta(x) \\ y = Cx \end{cases} \tag{60}$$

Combining d and ζ as in [39], Eq. (60) becomes:

$$\begin{cases} \dot{x} = Ax + Bu + F_a f_a + D_1 d_1 \\ y = Cx \end{cases} \tag{61}$$

where F_a is the first column of the matrix F_d, $D_1 = \begin{bmatrix} D & \Xi \end{bmatrix}$, and $d_1 = \begin{bmatrix} d \\ \zeta \end{bmatrix}$.

D and Ξ are chosen as:

$$D = \begin{bmatrix} \frac{1}{J_r} \\ 0 \\ 0 \\ 0 \\ 0 \end{bmatrix}, \quad \Xi = \begin{bmatrix} 0 \\ 0.01 \\ 0 \\ 0 \\ -0.02 \end{bmatrix}$$

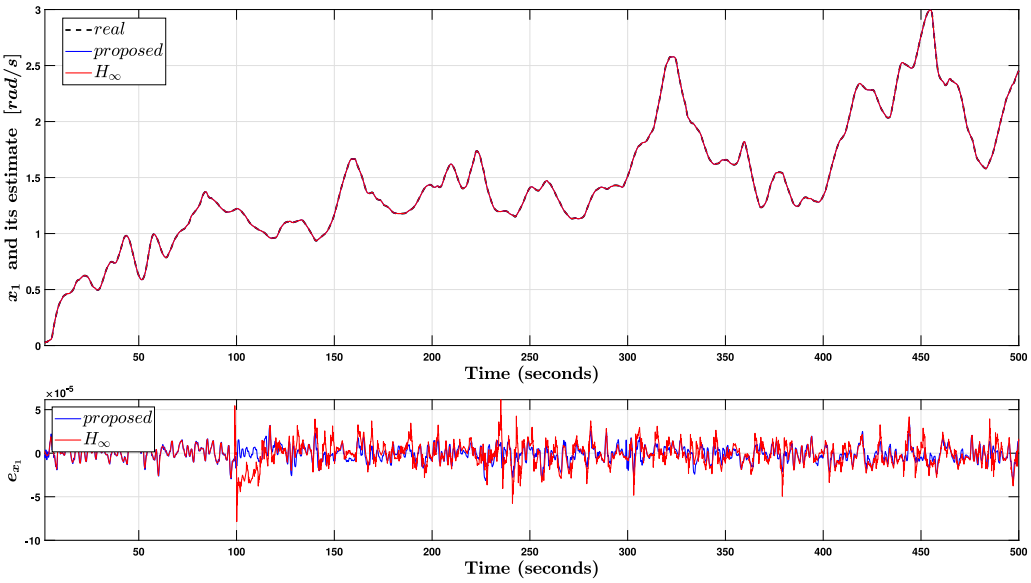

Fig. 3. System state x_1 and its estimate along with the variation of the estimation error (first case).

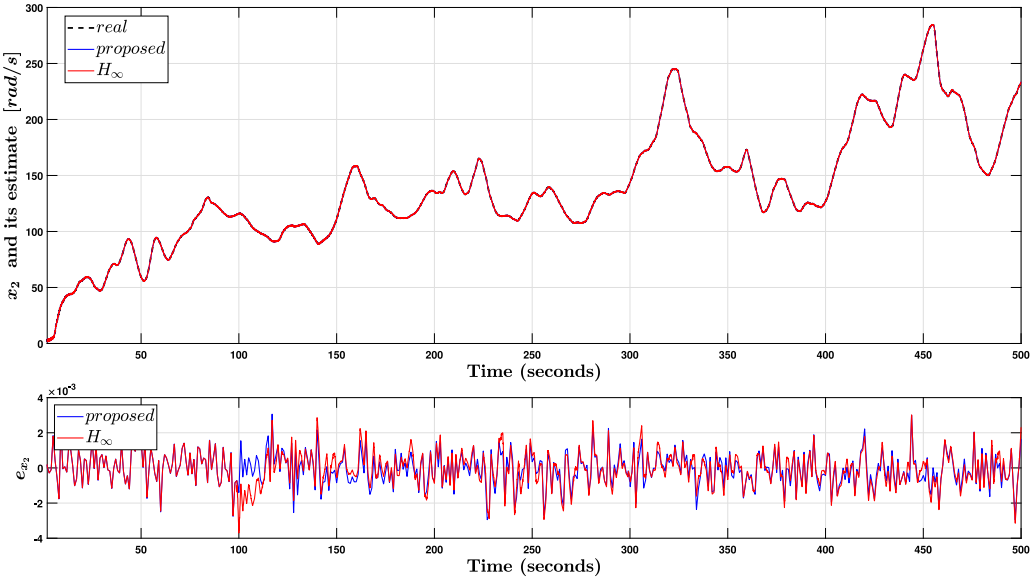

Fig. 4. System state x_2 and its estimate along with the variation of the estimation error (first case).

Table 3
Root mean square error between system states, actuator, and sensor faults with their estimation (second case).

Approach	x_1	x_2	x_3	x_4	x_5	f_a
H_∞	0.0000	**0.0006**	0.0000	0.0036	0.0187	81.5936
Proposed in [39]	0.0000	0.0830	0.0000	0.0057	0.0067	61.2897
Proposed	0.0000	0.0008	0.0000	**0.0015**	**0.0061**	**8.7031**

The disturbance $d(t)$ follows a Weibull distribution with the scale and shape parameters of respectively 10^2 and 10, starting from $t = 100$ s, as depicted in Fig. 10, and the uncertainties $\zeta = \begin{bmatrix}0.01 & 0 & 0.02\end{bmatrix} y$. And the actuator fault is considered as $f_a = 500 \times (u(t-80) - u(t-400))$.

In this simulation case, the results of the proposed approach are compared with the H_∞ technique as well as with the sliding mode observer for the actuator fault scenario proposed in [39]. The observer gain matrices of the three approaches are provided in Appendix B. Compared to H_∞ and the method described in [39], the suggested approach consistently shows superior accuracy in estimating the system states and actuator fault, as shown in Figs. 11 to 15. This demonstrates how successful the suggested method is for robust estimation. As it can be seen in Table 3, the proposed method produced the best results although the suggested strategy in [39] fared well when compared to H_∞.

6. Conclusion

In this paper, an Unknown Input Observer-based simultaneous states and faults estimation approach for wind turbine pitch and drive train systems is developed, which can effectively handle systems that are susceptible to disturbances and noises. The theoretical analysis of the proposed technique is well-defined. The design approach of a linear system estimator is satisfactorily provided and achieves robustness by using the Genetic Algorithm optimizer to minimize a multi-objective function derived from a set of performance indices in the frequency domain. The obtained results show great superiority of the developed technique compared with the H_∞ technique and the sliding mode observer.

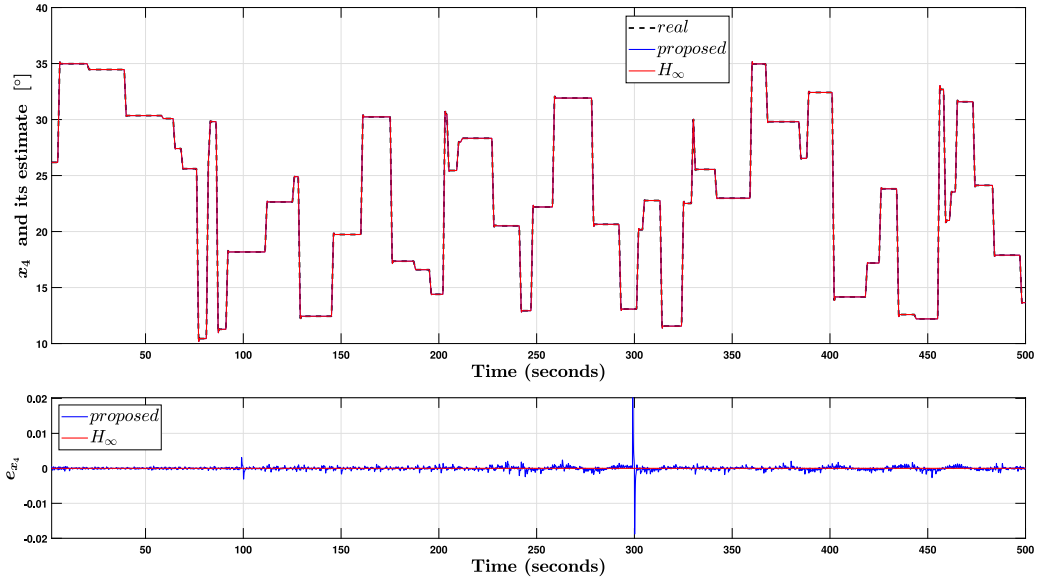

Fig. 5. System state x_4 and its estimate along with the variation of the estimation error (first case).

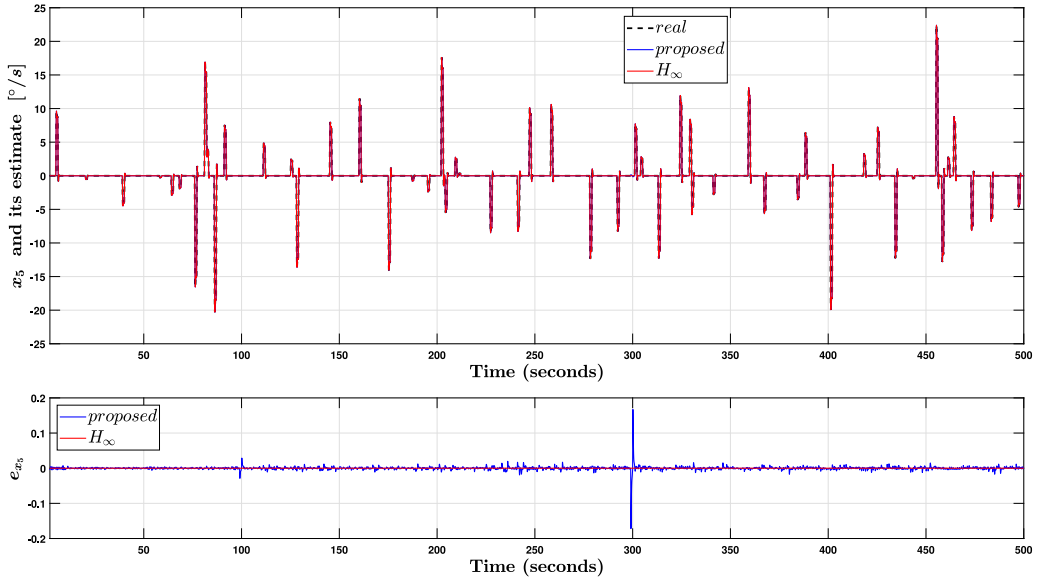

Fig. 6. System state x_5 and its estimate along with the variation of the estimation error (first case).

Declaration of competing interest

The authors declare that they do not have any financial or non-financial conflicts of interest.

Data availability

No data was used for the research described in the article.

Acknowledgment

This work was supported by Direction Générale de la Recherche Scientifique et Technologique under A01L08UN350120200002-PRFU.

Appendix A. Case 1

A.1. Proposed observer gain

$$K = \begin{bmatrix} 0.005 & 0.072 & 0.002 \\ -0.036 & 6.723 & -0.052 \\ 0.001 & 0.000 & 0.000 \\ 4.431 & 5.502 & 13.621 \\ -28.827 & -50.354 & -126.460 \\ 94083.466 & 124376.056 & 204032.291 \\ 2.140 & 0.178 & 0.606 \\ -29.492 & -28.969 & -69.962 \\ 15673.406 & 18767.128 & 29986.395 \\ 8.958 & 0.248 & 1.554 \\ -4.225 & -5.408 & -7.160 \end{bmatrix}$$

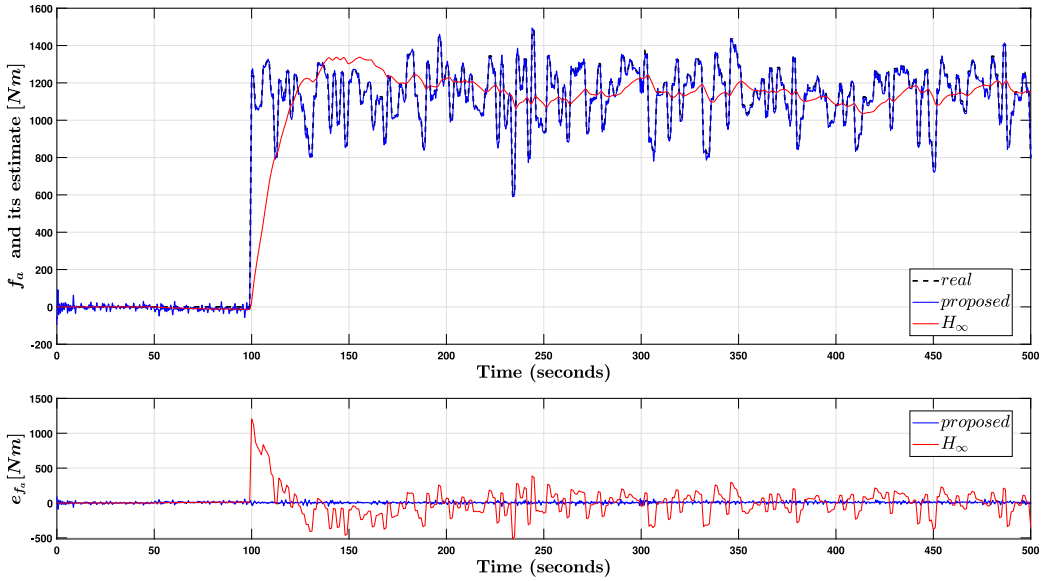

Fig. 7. Actuator fault and its estimate along with the variation of the estimation error e_{f_a} (first case).

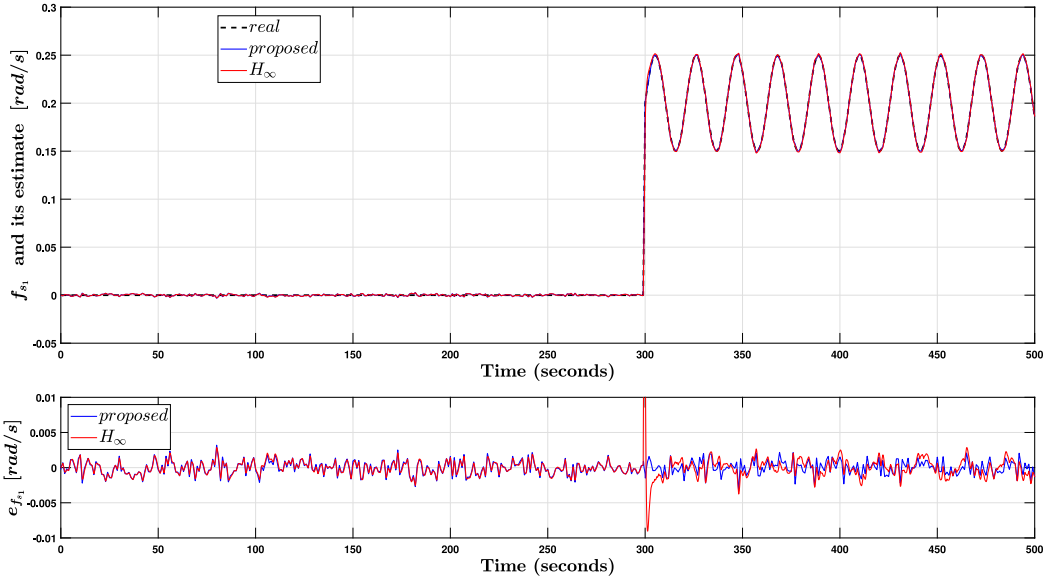

Fig. 8. First sensor fault and its estimate along with the variation of the estimation error $e_{f_{s_1}}$ (first case).

$$H = \begin{bmatrix} -0.001 & 0.001 & -0.000 \\ -0.030 & 1.006 & 0.001 \\ 0.000 & -0.000 & -0.000 \\ -2.151 & 0.860 & 0.066 \\ 19.210 & -8.038 & 5.470 \\ 15576.856 & -117395.993 & -3616.558 \\ 6.734 & 0.048 & 0.004 \\ 11.362 & -4.312 & 2.895 \\ 5467.725 & -21848.737 & -593.262 \\ 0.919 & 0.036 & 0.001 \\ 2.228 & -0.906 & 0.932 \end{bmatrix}$$

A.2. H_∞ observer gain

$$K = \begin{bmatrix} -0.000 & 0.097 & -0.000 \\ -0.009 & 9.215 & -0.000 \\ 0.000 & -0.000 & -0.000 \\ -0.000 & -0.000 & -0.000 \\ -0.000 & 0.000 & 0.000 \\ 0.120 & -126.174 & 0.000 \\ 0.606 & -0.020 & -0.000 \\ 0.000 & -0.000 & 0.632 \\ 3.917 & -4206.144 & 0.000 \\ 1.115 & -0.106 & -0.000 \\ -0.000 & -0.000 & 1.128 \end{bmatrix}$$

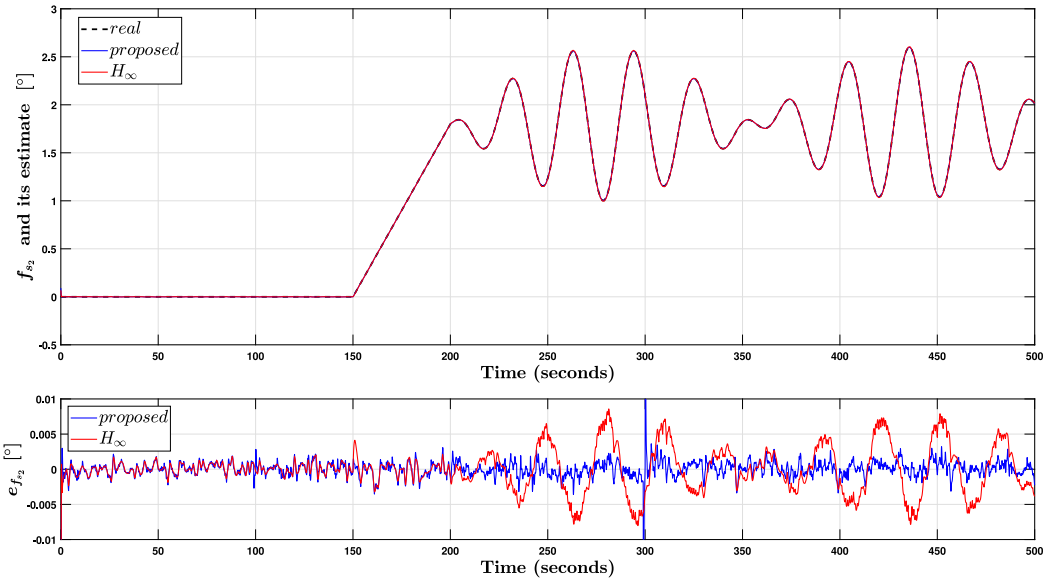

Fig. 9. Second sensor fault and its estimate along with the variation of the estimation error $e_{f_{s_2}}$ (first case).

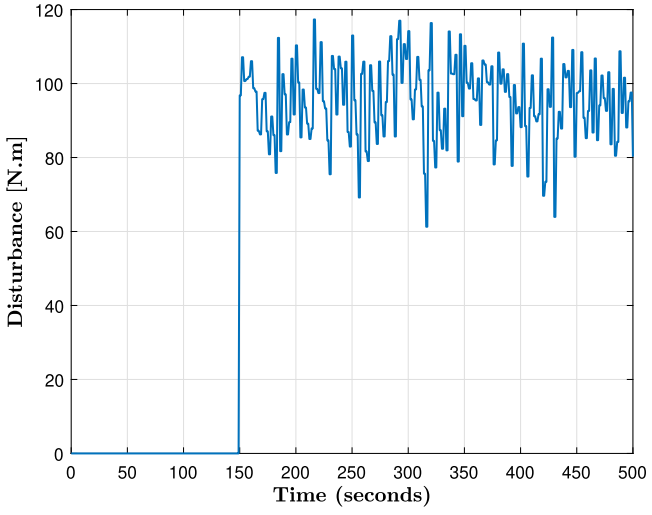

Fig. 10. Disturbance $d(t)$.

$$H = \begin{bmatrix} -0.000 & 0.010 & 0.000 \\ -0.023 & 0.869 & -0.000 \\ 0.000 & 0.000 & -0.000 \\ -0.000 & -0.000 & -0.000 \\ -0.000 & -0.000 & -0.000 \\ 0.259 & -12.454 & -0.000 \\ 1.113 & 0.009 & -0.000 \\ 0.000 & 0.000 & 1.190 \\ 8.557 & -413.179 & -0.000 \\ 0.607 & -0.009 & -0.000 \\ -0.000 & 0.000 & 0.653 \end{bmatrix}$$

Appendix B. Case 2

B.1. Proposed observer gain

$$K = \begin{bmatrix} 0.113 & 0.044 & 0.020 \\ 3.112 & 5.671 & 1.180 \\ 0.057 & 0.000 & 0.002 \\ -12.844 & -0.637 & 5.137 \\ 307.026 & 15.951 & -135.901 \\ 5332844.256 & 81558.741 & -82024.932 \\ 1485317.752 & 47522.134 & -9094.924 \end{bmatrix}$$

$$H = \begin{bmatrix} 0.488 & 0.002 & 0.004 \\ 2.560 & 0.970 & 0.181 \\ -0.084 & 0.000 & 0.001 \\ -10.740 & 0.095 & 0.597 \\ 306.400 & -2.408 & 1.116 \\ -6724910.896 & -8360.215 & 43603.483 \\ -3030140.228 & -6132.256 & 11460.276 \end{bmatrix}$$

B.2. H_∞ observer gain

$$K = \begin{bmatrix} 0.001 & 0.073 & -0.000 \\ 0.080 & 6.897 & 0.000 \\ -0.000 & -0.000 & 0.000 \\ -0.000 & 0.000 & 0.000 \\ 0.000 & -0.000 & -0.000 \\ -0.891 & -94.513 & 0.007 \\ -29.777 & -3152.188 & 0.226 \end{bmatrix}$$

$$H = \begin{bmatrix} 0.000 & 0.008 & 0.000 \\ 0.005 & 0.626 & -0.000 \\ -0.000 & 0.000 & -0.000 \\ -0.000 & 0.000 & -0.000 \\ -0.000 & -0.000 & 0.000 \\ -0.063 & -9.791 & -0.001 \\ -2.103 & -325.084 & -0.018 \end{bmatrix}$$

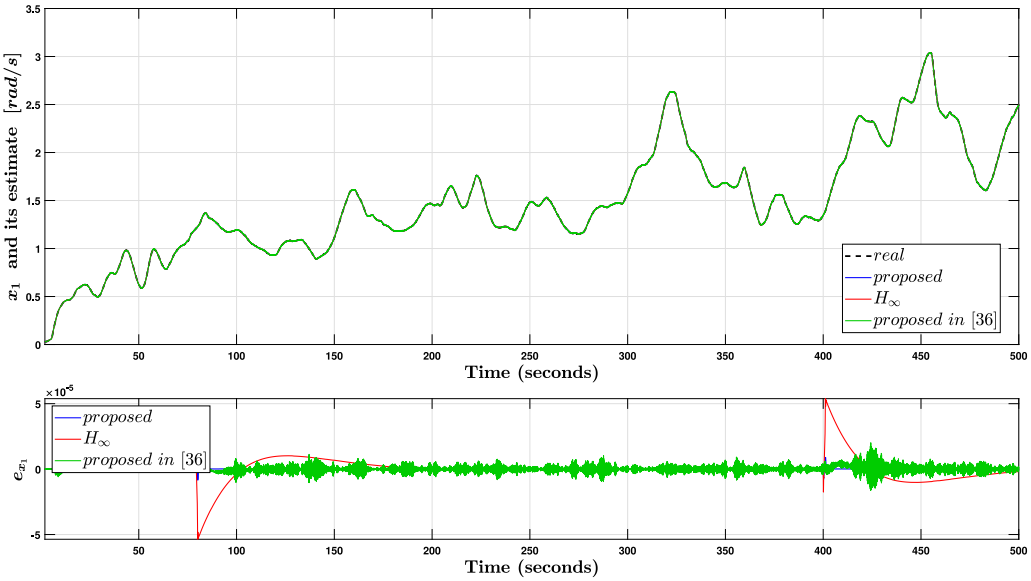

Fig. 11. System state x_1 and its estimate along with the variation of the estimation error (second case).

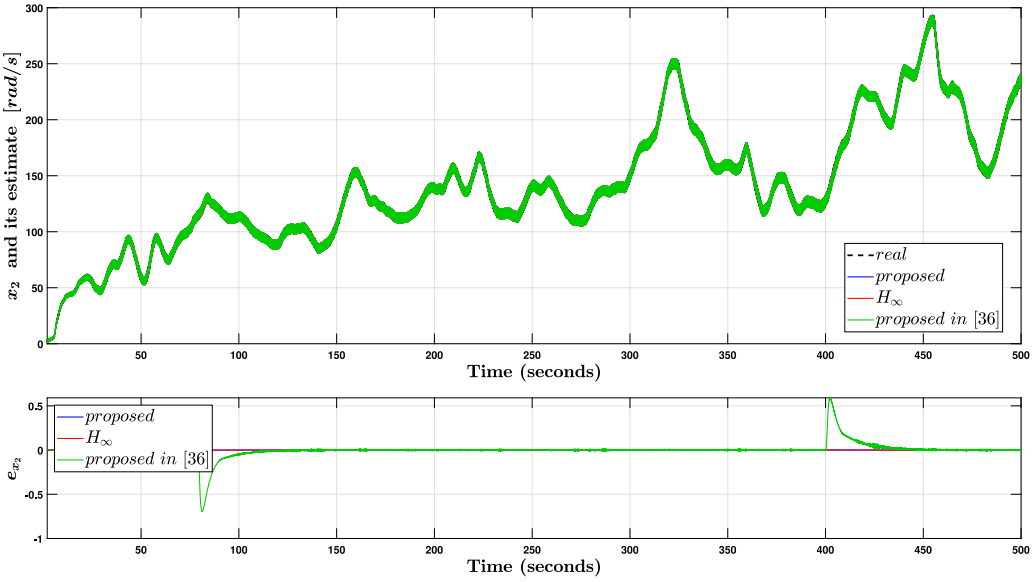

Fig. 12. System state x_2 and its estimate along with the variation of the estimation error (second case).

$$P = \begin{bmatrix} 11369810051.003 & 6658042.714 & 912629320.034 & -3917785.993 & -71776.013 \\ 6658042.714 & 4623.219 & 628164.284 & -2327.427 & -48.137 \\ 912629320.034 & 628164.284 & 1430534000.352 & -725970.255 & -24202.312 \\ -3917785.993 & -2327.427 & -725970.255 & 1043035387.806 & 23840.689 \\ -71776.013 & -48.137 & -24202.312 & 23840.689 & 76194611.702 \end{bmatrix}$$

Box II.

B.3. Sliding mode observer in [39] parameters

$\delta = 0.005$, $\Lambda = 0.1$, $\Gamma = 4$, $\sigma = 2$, $\mu = 0.2$ (see unnumbered equation in Box II).

$$L = \begin{bmatrix} 0.651 & -0.005 & -0.005 \\ 7901.093 & 8.350 & 5.094 \\ -64.051 & -0.011 & 0.021 \\ -0.017 & 0.000 & 1.091 \\ -0.021 & 0.000 & -106.120 \end{bmatrix}$$

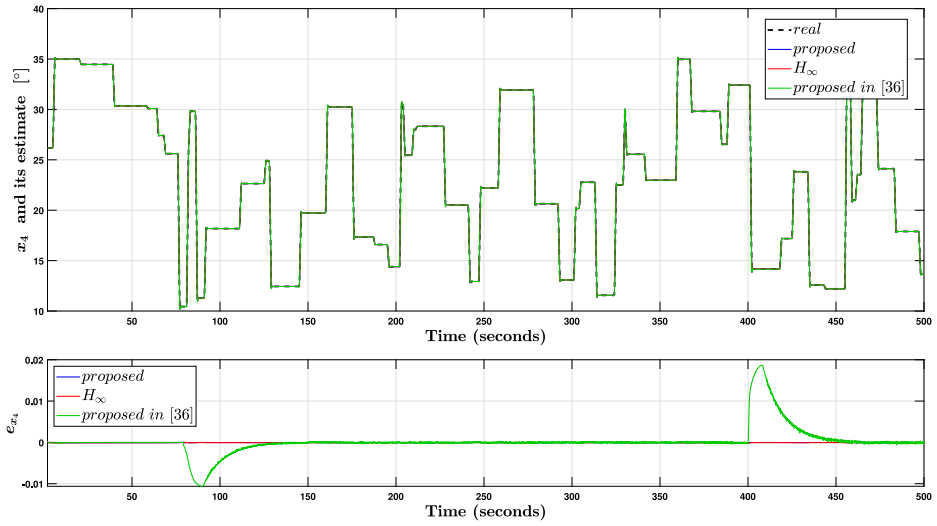

Fig. 13. System state x_4 and its estimate along with the variation of the estimation error (second case).

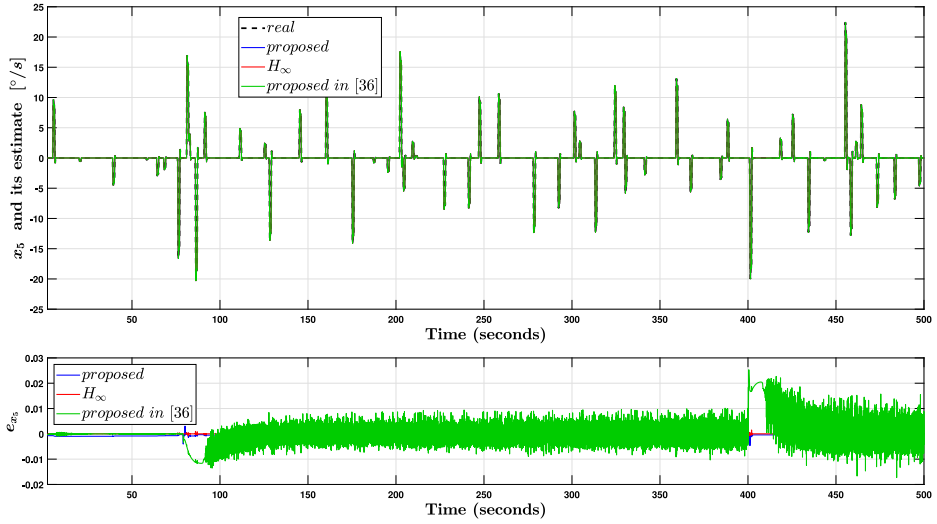

Fig. 14. System state x_5 and its estimate along with the variation of the estimation error (second case).

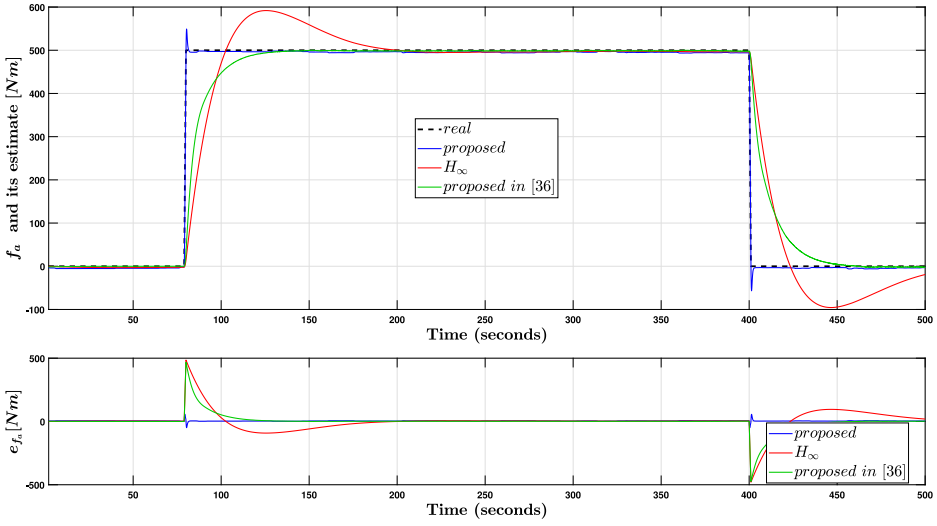

Fig. 15. Actuator fault and its estimate along with the variation of the estimation error e_{f_a} (second case).

$$K_1 = \begin{bmatrix} 206.724 & 0.121 & -0.071 \\ 68015.947 & 47.195 & -500.088 \end{bmatrix}$$

$$K_2 = \begin{bmatrix} -17071.904 & -11.854 & 5.968 \end{bmatrix}$$

References

[1] Khodabux K, Bhujun B, Chinnappa Naidu R, Dhawankar P, Busawon K. An overview on various faults of wind turbine parts. 2022.

[2] Rabaia MKH, Abdelkareem MA, Sayed ET, Elsaid K, Chae K-J, Wilberforce T, et al. Environmental impacts of solar energy systems: A review. Sci Total Environ 2021;754:141989. http://dx.doi.org/10.1016/j.scitotenv.2020.141989.

[3] Bojek P. Wind. 2023, https://www.iea.org/energy-system/renewables/wind. [Accessed 10 August 2023].

[4] Kavaz AG, Barutcu B. Fault detection of wind turbine sensors using artificial neural networks. J Sens 2018;2018:1–11. http://dx.doi.org/10.1155/2018/5628429.

[5] xing Yin X, gang Lin Y, Li W, jing Gu Y, jun Wang X, fei Lei P. Design, modeling and implementation of a novel pitch angle control system for wind turbine. Renew Energy 2015;81:599–608. http://dx.doi.org/10.1016/j.renene.2015.03.042.

[6] Ziyabari SHS, Shoorehdeli MA, Karimirad M. Robust fault estimation of a blade pitch and drivetrain system in wind turbine model. J Vib Control 2021;27(3–4):277–94. http://dx.doi.org/10.1177/1077546320926274.

[7] Azizi A, Nourisola H, Shoja-Majidabad S. Fault tolerant control of wind turbines with an adaptive output feedback sliding mode controller. Renew Energy 2019;135:55–65. http://dx.doi.org/10.1016/j.renene.2018.11.106.

[8] Shi F, Patton RJ. A robust adaptive approach to wind turbine pitch actuator component fault estimation. In: 2014 UKACC international conference on control. 2014, p. 468–73. http://dx.doi.org/10.1109/CONTROL.2014.6915185.

[9] Odgaard PF, Stoustrup J, Kinnaert M. Fault-tolerant control of wind turbines: A benchmark model. IEEE Trans Control Syst Technol 2013;21(4):1168–82. http://dx.doi.org/10.1109/TCST.2013.2259235.

[10] Zhang X, Zhang Q, Zhao S, Ferrari R, Polycarpou MM, Parisini T. Fault detection and isolation of the wind turbine benchmark: An estimation-based approach. IFAC Proc Vol 2011;44(1):8295–300. http://dx.doi.org/10.3182/20110828-6-IT-1002.02808, 18th IFAC World Congress.

[11] Asgari S, Yazdizadeh A. Robust model-based fault diagnosis of mechanical drive train in V47/660 kW wind turbine. Energy Syst 2018;9:921–52. http://dx.doi.org/10.1007/s12667-017-0231-2.

[12] Morato MM, Regner DJ, Mendes PRC, Normey-Rico JE, Bordons C. Fault analysis, detection and estimation for a microgrid via H_2/H_∞ LPV observers. Int J Electr Power Energy Syst 2019;105:823–45. http://dx.doi.org/10.1016/j.ijepes.2018.09.018.

[13] Du D, Cocquempot V, Jiang B. Robust fault estimation observer design for switched systems with unknown input. Appl Math Comput 2019;348:70–83. http://dx.doi.org/10.1016/j.amc.2018.11.034.

[14] Zhao X-Q, Dong Z, Wang Z, Li J. Simultaneous fault detection and control design for DC–AC converter with a neutral leg based on dynamic observer. Int J Electr Power Energy Syst 2022;143:108447. http://dx.doi.org/10.1016/j.ijepes.2022.108447.

[15] Wu Y, Du D, Liu B, Mao Z. Actuator fault estimation for two-stage chemical reactor system based on delta operator approach. J Process Control 2021;107:37–46. http://dx.doi.org/10.1016/j.jprocont.2021.09.013.

[16] Morato MM, Mendes PRC, Normey-Rico JE, Bordons C. Robustness conditions of LPV fault estimation systems for renewable microgrids. Int J Electr Power Energy Syst 2019;111:325–50. http://dx.doi.org/10.1016/j.ijepes.2019.04.014.

[17] Alaei HK, Yazdizadeh A. A new robust H_∞ sliding mode observer-based state estimation and fault reconstruction for nonlinear uncertain boiler system. Soft Comput 2016;21(14):3957–68. http://dx.doi.org/10.1007/s00500-016-2046-9.

[18] Tavasolipour E, Poshtan J, Shamaghdari S. A new approach for robust fault estimation in nonlinear systems with state-coupled disturbances using dissipativity theory. ISA Trans 2021;114:31–43. http://dx.doi.org/10.1016/j.isatra.2020.12.040.

[19] Kazemi MG, Montazeri M. A new fault detection approach for nonlinear Lipschitz systems with optimal disturbance attenuation level and Lipschitz constant. Electr Eng 2018;100(3):1997–2009. http://dx.doi.org/10.1007/s00202-018-0680-1.

[20] Abbaszadeh M, Marquez HJ. Robust h observer design for a class of nonlinear uncertain systems via convex optimization. In: 2007 American control conference. IEEE; 2007, p. 1699–704. http://dx.doi.org/10.1109/ACC.2007.4282280.

[21] Ichalal D, Marx B, Ragot J, Maquin D. Fault detection, isolation and estimation for Takagi–Sugeno nonlinear systems. J Franklin Inst B 2014;351(7):3651–76. http://dx.doi.org/10.1016/j.jfranklin.2013.04.012.

[22] Zhang K, Liu G, Jiang B. Robust unknown input observer-based fault estimation of leader–follower linear multi-agent systems. Circuits Systems Signal Process 2016;36(2):525–42. http://dx.doi.org/10.1007/s00034-016-0313-8.

[23] Yan X-G, Edwards C. Nonlinear robust fault reconstruction and estimation using a sliding mode observer. Automatica 2007;43(9):1605–14. http://dx.doi.org/10.1016/j.automatica.2007.02.008.

[24] Park T-G, Ryu J-S, Lee K-S. Actuator fault estimation with disturbance decoupling. IEEE Proc D 2000;147(5):501–8. http://dx.doi.org/10.1049/ip-cta:20000639.

[25] Gao Z, Liu X, Chen M. Unknown input observer based robust fault estimation for systems corrupted by partially-decoupled disturbances. IEEE Trans Ind Electron 2015;1. http://dx.doi.org/10.1109/tie.2015.2497201.

[26] Lan J, Patton RJ. A decoupling approach to integrated fault-tolerant control for linear systems with unmatched non-differentiable faults. Automatica 2018;89:290–9. http://dx.doi.org/10.1016/j.automatica.2017.12.011.

[27] Lan J. Asymptotic estimation of state and faults for linear systems with unknown perturbations. Automatica 2020;118:108955. http://dx.doi.org/10.1016/j.automatica.2020.108955.

[28] Lan J, Patton R. Asymptotic estimation of state, fault and perturbation for nonlinear systems and its fault-tolerant control application. Int J Control Autom Syst 2021;19(3):1175–82. http://dx.doi.org/10.1007/s12555-019-1078-1.

[29] Rahnavard M, Ayati M, Hairi Yazdi MR, Mousavi M. Finite time estimation of actuator faults, states, and aerodynamic load of a realistic wind turbine. Renew Energy 2019;130:256–67. http://dx.doi.org/10.1016/j.renene.2018.06.053.

[30] Sloth C, Esbensen T, Stoustrup J. Robust and fault-tolerant linear parameter-varying control of wind turbines. Mechatronics 2011;21(4):645–59. http://dx.doi.org/10.1016/j.mechatronics.2011.02.001.

[31] Wang X, Shen Y. Fault tolerant control of DFIG-based wind energy conversion system using augmented observer. Energies 2019;12(4). http://dx.doi.org/10.3390/en12040580.

[32] Witczak M, Rotondo D, Puig V, Nejjari F, Pazera M. Fault estimation of wind turbines using combined adaptive and parameter estimation schemes. Internat J Adapt Control Signal Process 2018;32(4):549–67. http://dx.doi.org/10.1002/acs.2792.

[33] Odofin S, Bentley E, Aikhuele D. Robust fault estimation for wind turbine energy via hybrid systems. Renew Energy 2018;120:289–99. http://dx.doi.org/10.1016/j.renene.2017.12.031.

[34] Liu Y, Patton RJ, Shi S. Actuator fault tolerant offshore wind turbine load mitigation control. Renew Energy 2023;205:432–46. http://dx.doi.org/10.1016/j.renene.2023.01.092.

[35] Chen J, Patton RJ, Liu G-P. Optimal residual design for fault diagnosis using multi-objective optimization and genetic algorithms. Internat J Systems Sci 1996;27(6):567–76. http://dx.doi.org/10.1080/00207729608929251.

[36] Burrows SP, Patton RJ. Design of a low-sensitivity, minimum norm and structurally constrained control law using eigenstructure assignment. Optim Control Appl Methods 1991;12(3):131–40. http://dx.doi.org/10.1002/oca.4660120302.

[37] Liang X, Wang Q, Hu C, Dong C. Observer-based H_∞ fault-tolerant attitude control for satellite with actuator and sensor faults. Aerosp Sci Technol 2019;95:105424. http://dx.doi.org/10.1016/j.ast.2019.105424.

[38] Zhang F. The Schur complement and its applications, vol. 4. Springer Science & Business Media; 2006.

[39] Taherkhani A, Bayat F. Wind turbines robust fault reconstruction using adaptive sliding mode observer. IET Gener Transm Distrib 2019;13(14):3096–104. http://dx.doi.org/10.1049/iet-gtd.2018.6736.